Available online at www.sciencedirect.com
SCIENCE DIRECT
Solid State Communications 138 (2006) 64–67
solid state communications
www.elsevier.com/locate/ssc

Influence of carbon concentration on structural, magnetic and electrical transport properties for antiperovskite compounds AlC_xMn_3

P. Tong, Y.P. Sun *, B.C. Zhao, X.B. Zhu, W.H. Song

Key Laboratory of Materials Physics, Institute of Solid State Physics, Chinese Academy of Sciences, Hefei 230031, People's Republic of China

Received 23 August 2005; received in revised form 20 December 2005; accepted 13 February 2006 by T.T.M. Palstra
Available online 3 March 2006

Abstract

The structural, magnetic and transport properties of the antiperovskite AlC_xMn_3 ($1.0 \leq x \leq 1.4$) are investigated. It is found that the lattice parameter a increases monotonously with nominal carbon concentration x. The Curie temperature T_C increases with increasing x from 1.0 to 1.1 and then decreases with further increasing x. The highest T_C value is 364 K, about 70 K higher than that of stoichiometric $AlCMn_3$ reported previously. This may be attributed to a competition between the lattice expansion and the strong Mn 3d–C 2p hybridization. Below 100 K, the resistivity can be well described as $\rho(T)=\rho_0+AT^2$, corresponding to the electron–electron scattering. A increases with x, suggesting certain changes in the electronic structure, e.g. carrier density. Above 250 K, all $\rho(T)$ curves depart from the linear dependence on temperature and seem to take on a tendency towards saturation.

PACS: 75.50.Cc; 75.10.Lp

Keywords: A. Metals; A. Magnetically ordered materials; D. Electronic band structure; D. Electronic transport

1. Introduction

Over the past several decades, oxygen-based perovskite compounds with general formula RMO_3 (R, rare earth or alkaline element; M, transition metal) have been studied extensively, because they exhibit a wide range of novel phenomena such as high superconducting transition temperature [1], ferroelectrics [2] and colossal magnetoresistance [3]. In contrast, relatively little is known about the antiperovskite materials AXM_3 (A, main group element; X, carbon, boron or nitrogen; M, transition metal). In 2001, the discovery of superconductivity in $MgCNi_3$ [4] led to renewed interest in this type of compounds. Up to the present, many interesting properties, such as giant magnetoresistance [5], large negative magnetocaloric effect [6], a nearly zero temperature coefficient of resistance [7], and magnetic ordering induced cracks [8] have been reported in the antiperovskite compounds. Among the family of carbide antiperovskites, $AlCMn_3$ is a ferromagnetic (FM) compound with a Curie temperature (T_C) of 293 K [9]. Except for a few early studies focused on magnetic structure and properties [9,10], little is known of $AlCMn_3$. Furthermore, for the carbide antiprovskite materials, the physical properties are of seriously carbon concentration dependent [10,11]. Therefore, in this paper we aimed at the influence of carbon content x on the structural, magnetic and transport properties of AlC_xMn_3. It is found that all of them are sensitive to the carbon content x in various ways.

2. Experimental details

The samples with nominal composition AlC_xMn_3 ($x=1.0$, 1.1, 1.2, 1.3, 1.4) were prepared by arc melting in a cold copper crucible under purified argon atmosphere. Before arc-melting, the initial powers (Al, Graphite, and Mn) with high purity were thoroughly mixed and pressed into pellets. To improve the homogeneity the as-melted samples were annealed in evacuated quartz tubes at 900 °C for 4 days. X-ray powder diffraction patterns were collected using a Philips X'pert PRO X-ray diffractometer with Cu Kα radiation at room temperature and refined using a standard Rietveld technique. The magnetic measurements were carried out with a quantum design superconducting quantum interference device (SQUID) MPMS system ($2\ K \leq T \leq 400\ K$, $0 \leq H \leq 50$ kOe). The

* Corresponding author. Address: Key Laboratory of Materials Physics, Institute of Solid State Physics, Chinese Academy of Sciences, P.O. Box 1129, Hefei 230031, China. Tel.: +86 551 559 1436; fax: +86 551 559 1434.
E-mail address: ypsun@issp.ac.cn (Y.P. Sun).

0038-1098/$ - see front matter © 2006 Elsevier Ltd. All rights reserved.
doi:10.1016/j.ssc.2006.02.009

resistance was measured by the standard four-probe method in a commercial quantum design physical property measurement system (PPMS) ($2\ \mathrm{K} \leq T \leq 400\ \mathrm{K}$, $0 \leq H \leq 90\ \mathrm{kOe}$).

3. Results and discussion

Fig. 1 shows the X-ray diffraction (XRD) patterns of AlC_xMn_3 samples. Except for a small amount of unreacted graphite detected as a secondary phase in samples with $x = 1.3$ and 1.4, single-phase samples were obtained, which have the cubic perovskite structure with the space group $Pm3m$. As a result of structural refinement, the lattice parameter a is found to increase linearly with x. The largest value of a is 0.3872(0) nm for the sample with $x = 1.4$, which is similar to that of the stoichiometric $AlCMn_3$ (0.3871 nm) [9]. Thus, the samples with $x < 1.4$ are carbon deficient, the extent to which increases with decreasing x. This can be understood as follow: with increasing the nominal carbon content x, more carbon atoms enter into the body-centered position of AlC_xMn_3 unit cells, leading to the expansion of lattice, and the excess carbon was lost during the arc melting process [12].

Fig. 2 shows the temperature dependence of the magnetization $M(T)$ under the zero-field cooling (ZFC) mode in an applied field of 100 Oe. With decreasing temperature, all samples exhibit a sharp paramagnetic (PM) to FM transition. As can be seen from Fig. 3, for all samples the temperature dependence of the inverse of magnetic susceptibility χ above T_C can be well described by the Curie–Weiss law, $1/\chi = (T - \theta)/C$, where θ and C are the Curie–Weiss temperature and Curie constant, respectively. Based on Curie constant $C = N_0\mu_{\mathrm{eff}}^2/3k_B$, where k_B, N_0, μ_{eff} are Boltzmann constant, Avogadro's constant and effective magnetic moment respectively, μ_{eff} can be deduced [13]. For the reason of clarity, the nominal carbon content x dependences of the Curie temperature T_C (defined as the inflection point of dM/dT), μ_{eff} and lattice parameter a are plotted in Fig. 4(a)–(c), respectively. It can be clearly seen that T_C increases initially with x and reaches the highest value 364 K at $x = 1.1$, which is about 70 K higher than the value of the stoichiometric $AlCMn_3$ [9]. As $x > 1.1$, T_C decreases with further increasing x. The variation of μ_{eff} is

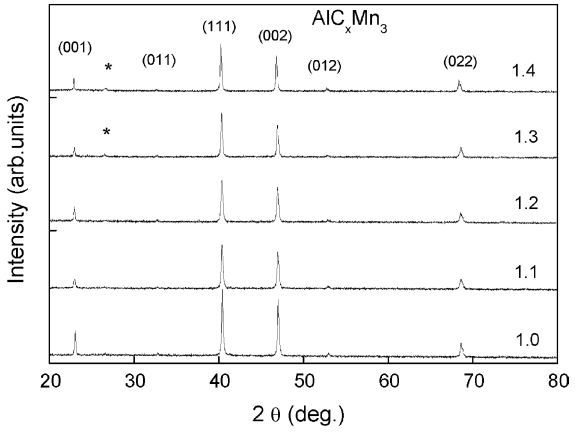

Fig. 1. XRD patterns for AlC_xMn_3. Asterisks indicate the diffraction peaks of unreacted graphite.

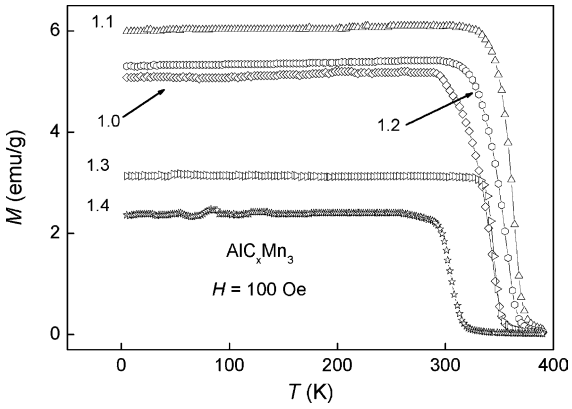

Fig. 2. Zero field cooling (ZFC) magnetization as a function of temperature measured in a magnetic field of 100 Oe for AlC_xMn_3.

similar to that of T_C, whereas a shows a linear dependence on x. However, for its counterpart GaC_xMn_3, there is no such a 'peak' in T_C vs. x (carbon content) curve. Instead the Curie temperature T_C decreases with increasing x in the whole range carbon content studied [10].

Previous theoretical studies commented that, for Mn-based carbide antiperovskites, the general features of the band structure could be briefly summarized as follows: the density of states (DOS) at the Fermi level E_F, $N(E_F)$, is predominantly due to Mn 3d electrons [14]. In addition, there exists a strong hybridization of Mn 3d states with C 2p states, which widens the bandwidth of Mn 3d states, thus the itinerant magnetic mechanism is established [15]. In this experiment, the increase of T_C and μ_{eff} in the low carbon content region can be interpreted readily by the increase in lattice parameter. Namely, the lattice expansion leads to the narrowing of bandwidth [16], and accordingly to an increase of $N(E_F)$. It will lead to an increase in both T_C and μ_{eff} as predicted by the Stoner model for itinerant ferromagnetism [17]. On the other hand, however, with more interstitial carbon atoms entering into the body centered positions, which are the nearest neighbors of Mn atoms, the C 2p–Mn 3d hybridization will become stronger and give rise to the broadening of bandwidth, and accordingly to a

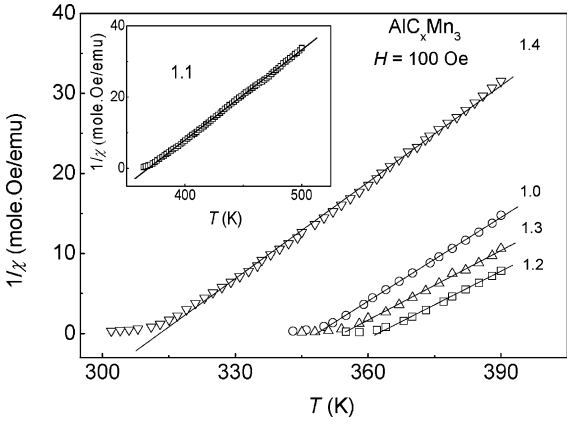

Fig. 3. The temperature dependence of the inverse of the magnetic susceptibility above T_C, χ^{-1} for AlC_xMn_3 compounds. The solid lines are fits to the Curie–Weiss equation. Inset: for the reason of clarity, data for $x = 1.0$ was measured up to 500 K using VSM with oven in PPMS system.

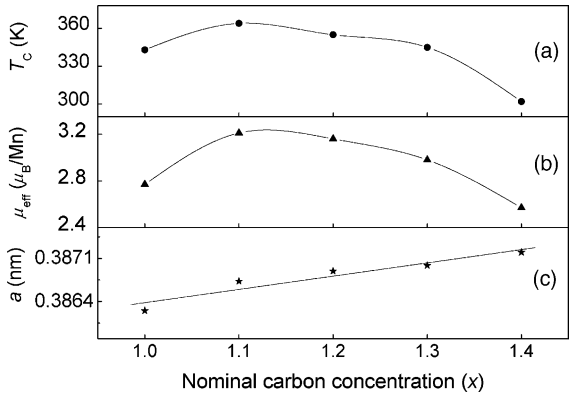

Fig. 4. (a)–(c) are the dependences of Curie temperature T_C, effective magnetic moment μ_{eff} and lattice parameter a of AlC_xMn_3 on nominal carbon content x, respectively. Solid lines are guides to the eye.

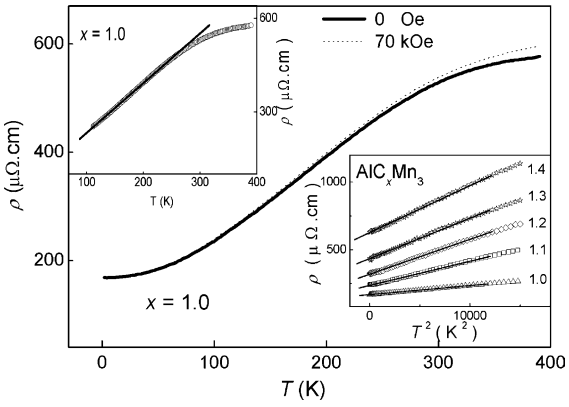

Fig. 6. $\rho(T)$ curves for sample $x=1.0$ under the magnetic fields of both zero and 70 kOe. Left inset: linear fit of resistivity data for sample $x=1.0$ between 100 and 250 K; right inset: low temperature resistivity plotted as $\rho(T)$ vs. T^2. Solid lines are linear fits.

decline in $N(E_F)$. Therefore, it is considered that with increasing carbon content from the beginning concentration $x=1.0$, the effect of hybridization on $N(E_F)$ becomes more and more prominent and comparable with that of the lattice expansion at the concentration $x=1.1$. After this concentration, the strong hybridization is responsible for the attenuation of $N(E_F)$, hence a suppression in T_C and μ_{eff}.

Fig. 5 shows the temperature dependence of the resistivity for AlC_xMn_3 at zero magnetic field in the temperature range of 5–390 K. All samples exhibit metallic behavior in the whole temperature range studied. The low temperature resistivity can be well fitted with the formula, $\rho=\rho_0+AT^2$ (see right inset of Fig. 6), where ρ_0 and A are the residual resistivity and coefficient for the quadratic term, respectively. For the sake of comparison, the temperature range for fitting was restricted between 5 and 100 K for all samples. The variations of fitted ρ_0 and A with x are shown in Fig. 7. Both of them exhibit roughly linear dependence on x. We note that the contribution to ρ_0 from the unreacted graphite could not be ignored, especially for high carbon content samples. As for the coefficient A, no obvious change ($<0.5\%$) is found under a magnetic field of 70 kOe, thereby the quadratic behavior of resistivity in this experiment should not be attributed to the spin fluctuations [18] or electron–magnon scattering [19]. Alternatively, the general

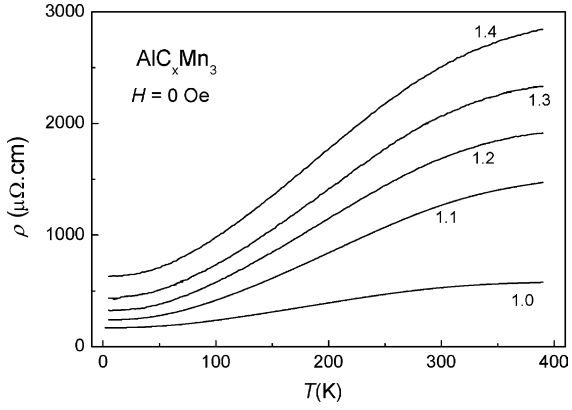

Fig. 5. Temperature dependence of resistivity for AlC_xMn_3 at zero magnetic field in the temperature range of 5–390 K.

electron–electron (e–e) scattering mechanisms within the Fermi liquid model, giving a T^2 dependence of the resistivity, which is insensitive to magnetic field [20], may be applicable here. As suggested in Ref. [21], the magnitude of e–e scattering should have a dependence on the carrier concentration n as $n^{-5/3}$. The increase in A with increasing x is suggestive of the decrease of carrier concentration, which possibly accounts for the increase of ρ_0. Given a three-dimensional Fermi surface in AlC_xMn_3, the DOS at E_F, $N(E_F)$ would be proportional to $n^{1/3}$ [22]. Thus the relation between $N(E_F)$ and the coefficient for quadratic term, A can be simply written as $N(E_F)\sim A^{-1/5}$. According to this relation, the increase in A as x increases from 1.1 to 1.4 may correspond to the decrease of $N(E_F)$, which leads to the suppression of T_C. However, as x increases from 1.0 to 1.1, this simple model seems to be unreasonable, because the increase in $N(E_F)$ is expected to be responsible for the increase of T_C. Thus this model is too simple to completely explain the behavior of A. Commonly the mechanism of e–e scattering is related to many aspects of the electronic structure, such as the carrier density [22], Fermi energy [22], renormalization of the electron effective mass [23], configuration of Fermi surface [24], and so on. The variation of A with x is probably due to the cooperative effect of the above ingredients, since they are associated with each other.

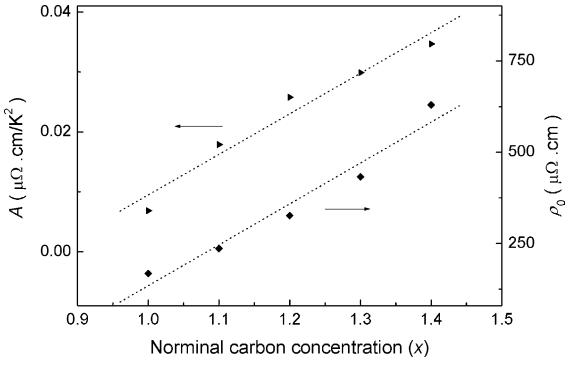

Fig. 7. The values of the residual resistivity ρ_0 and the quadratic term coefficient A plotted as a function of nominal carbon content x. The dotted lines are just guides to eye.

Within the temperature range from 100 to about 250 K, $\rho(T)$ curves are linearly dependent on temperature, which can be identified as the electron–phonon scattering [25] (left inset of Fig. 6). Above about 250 K all $\rho(T)$ curves deviate from linearity with a tendency towards saturation ($d^2\rho(T)/dT^2<0$). It happens near the region of T_C, at which a maximum in $d\rho(H=0)/dT$ is expected for FM metals due to the spin disorder [26]. In this experiment there are no anomalies in this region in the $d\rho(H=0)/dT$ vs. T curves. Furthermore, as shown in Fig. 6, the resistivity in this region is slightly increased at a magnetic field of 70 kOe. Therefore, the spin disorder model is incapable of explaining the deviation of resistivity from linearity. Similar resistivity saturation has been investigated in many metals, especially in A15 superconductors [27]. It has been interpreted in terms of the so-called Mott-Ioffe-Regel limit (MIRL) model [28]. Namely, if the electron–phonon scattering is the dominant mechanism for temperature dependent resistivity, and the mean free path of conduction electron (l) is as short as the order of a few inter-atomic spacing (a), i.e. $l\sim a$, a tendency towards saturation in resistivity will be expected. Since, we do not have resistivity data at higher temperatures, it is difficult to conclude whether the MIRL model is applicable or not. In order to shed a light on the nature of the open issues mentioned above, further experimental efforts, e.g. the measurements of specific heat and Hall effect are needed. Besides, we hope that this paper will trigger theoretical calculations aimed at the electronic structure of this system, which are essential to a better understanding of the nature of $AlCMn_3$ but short of reports up to now.

4. Conclusions

In summary, the influence of carbon content on the structural, magnetic and electrical transport properties of antiperovskite compounds AlC_xMn_3 have been investigated. The lattice is found to expand with the increase of x. The Curie temperature T_C and effective magnetic moment μ_{eff} increase initially and then decrease with increasing x, which is presumably due to the competition between the lattice expansion and the Mn 3d–C 2p hybridization. The transport behavior is suggested to originate from the electron–electron scattering (T^2 term) and electron–phonon scattering (linear term) for $5\ K<T<100\ K$ and $100<T<250\ K$, respectively. The coefficient of the T^2 term increases with x, which is possibly connected with certain changes in the electronic structure. When $T>250$ K, the resistivity of all samples exhibits a tendency towards saturation, which appears to have nothing to do with the spin disorder in the vicinity of T_C.

Acknowledgements

This work is supported by the National Key Basic Research under Contract No. 001CB610604, and the National Nature Science Foundation of China under Contract 10474100, and Fundamental Bureau of Chinese Academy of Sciences. We would like to thank Dr J.L. Wang for many helpful discussions.

References

[1] J.G. Bednorz, et al., Z. Phys. B: Condens. Matter 64 (1986) 189.
[2] C.H. Ahn, et al., Science 276 (1997) 1100.
[3] E.L. Nagaev, Phys. Rep. 346 (2001) 388.
[4] T. He, et al., Nature (London) 411 (2001) 54.
[5] K. Kamishima, et al., Phys. Rev. B. 63 (2000) 024426.
[6] T. Tohei, et al., J. Appl. Phys. 94 (2003) 1800.
[7] E.O. Chi, et al., Solid State Commun. 120 (2001) 307.
[8] W.S. Kim, et al., Phys. Rev. B. 68 (2003) 172402.
[9] A. Kenmotsu, et al., J. Phys. Soc. Jpn. 32 (1972) 377.
[10] D. Fruchart, et al., J. Phys. Soc. Jpn. 44 (1978) 781.
[11] D. Fruchart, et al., J. Solid State 8 (1973) 182.
[12] R.E. Schaak, et al., J. Solid State Chem. 177 (2004) 1244.
[13] E.M. Levin, et al., J. Appl. Phys. 96 (2004) 5085.
[14] K. Motizuki, et al., J. Phys. C: Solid State Phys. 21 (1988) 5251.
[15] J.H. Shim, et al., Phys. Rev. B. 66 (2002) 020406 (R).
[16] M.S. Park, et al., Supercond. Sci. Technol. 17 (2004) 274.
[17] K.G. Efthimiadis, et al., J. Magn. Magn. Mater. 162 (1996) 259.
[18] M. Yoshizawa, et al., J. Phys. Soc. Jpn. 61 (1992) 3313.
[19] M.B. Salamon, et al., Rev. Mod. Phys. 73 (2001) 583.
[20] L.M. Wang, et al., Phys. Rev. B. 70 (2004) 014433.
[21] N. Tralshawala, et al., Phys. Rev. B. 44 (1991) 12102.
[22] P.C. Klipstein, et al., J. Phys. C: Solid State Phys. 14 (1981) 4067.
[23] S.Y. Li, et al., Phys. Rev. Lett. 93 (2004) 056401.
[24] J. Arout Chelvanea, et al., J. Magn. Magn. Mater. 277 (2004) 175.
[25] M. Zhang, et al., J. Magn. Magn. Mater. 278 (2004) 328.
[26] M.E. Fisher, et al., Phys. Rev. Lett. 20 (1968) 665.
[27] D.W. Woodard, et al., Phys. Rev. 136 (1964) A166.
[28] G. Cao, et al., Solid State Commun. 131 (2004) 331.